AIRCRAFT HYDRO-MECHANICAL NOZZLE VERSUS PNEUMO-HYDRAULIC NOZZLE AS CONTROLLED OBJECTS

Alexandru - Nicolae TUDOSIE

University of Craiova, Romania (atudosie@elth.ucv.ro)

DOI: 10.19062/2247-3173.2023.24.23

Abstract: *The paper makes a comparison between two types of automatic control systems for the opening of the exhaust nozzle as objects subject to automatic control, under the conditions of their use on various types of jet engines for aircraft. Mathematical models of these nozzles are issued and some possible control schemes are described; Matlab-Simulink simulations are performed concerning object(s) step responses for throttle's step input. Some conclusions are drawn and some comments concerning the properties and the quality of the studied systems were also presented.*

Keywords: *exhaust, nozzle, jet-engine, speed, actuator, step input, control.*

1. INTRODUCTION

An exhaust nozzle (EN) for propulsion use is a special conceived device, designed to control the direction and the speed of a fluid flow as it exits a combustion chamber or a turbine [1]. When used on aircraft applications, the EN is also known as propelling nozzle and converts the energy of hot gases into propulsive force (thrust), so the engine becomes a jet engine, according to the classification given in [2].

Jet engines' nozzles accelerate the hot gases flow, depending on engine's power setting, to subsonic, transonic or supersonic velocity. This velocity depends on nozzle's internal shape, as well as on pressure distribution at its entry, respectively at its exit [2], [3].

Nowadays used nozzles have convergent or convergent-divergent (de Laval) shape, according to its purpose; convergent nozzles can only ensure subsonic exhaust velocities, at most sonic velocities, while de Laval nozzles can accelerate gas flow within their divergent sections to supersonic velocities ([2], [3], [4]).

In terms of their exhaust area, nozzles may have a fixed geometry, or they may have variable geometry ([2], [3]); variable geometry assures different exit areas, in order to control the operation of the engine [5]. This kind of nozzle is mandatory when the jet engine is fitted with an afterburner, for supersonic flights. When a jet-engine with afterburning is equipped with a de Laval nozzle, the variable area is its throat; however, for high supersonic flight speeds (when high nozzle pressure ratios are obtained), nozzles might have variable area divergent sections too ([2], [3]).

Most of nowadays in use propulsion nozzles are convergent. If nozzle's pressure ratio is above the critical value, the nozzle will choke [1] and the expansion to atmospheric pressure takes place downstream (in the jet wake) and the propulsion force is weaker, based on the imbalance between the exhaust area static pressure and the atmospheric pressure ([1], [2]).

Most of subsonic engines have nozzles of a fixed size because the changes in engine performance with altitude and subsonic flight speeds are acceptable with such architecture. However, high performance subsonic engines (e.g. multi-spool engines) and all supersonic engines employ variable architecture [2], consisting of a series of moving, overlapping petals (flaps) which build a nearly circular nozzle cross-section ([2], [3]), because of afterburner's requests, to prevent adversely affecting the operation of the jet-engine.

The nozzle opening control is carried out by various methods and is provided by control equipment based on various principles (mechanical, hydraulic, pneumatic, electrical or combinations thereof), generically called exhaust nozzle's control units (ENCU). The decision is taken by the engine designer in correlation with the designer of the aircraft that the engine is going to equip. Consequently, it is important that the decision be taken considering as many aspects as possible, including the behavior of the aircraft-engine-nozzle assembly as an object subject to automatic control and to estimate the advantages and disadvantages of using a certain type of exhaust nozzle.

2. PROBLEM FORMULATION

The paper intends to make a comparison between two types of automatic control systems for the opening of the exhaust nozzle as objects subject to automatic control, under the conditions of their use on various types of jet engines for aircraft. In fact, the direct comparison between the two types of ENCU cannot be always relevant; it is important to compare the effects of using each ENCU in an embedded control architecture of the same jet-engine, be it single-spool single-jet engine, double-spool single-jet engine or low by-pas turbofan.

The ENCU embedding into engine's control system entails some consequences concerning some modifications of engine's behavior as controlled object, such as its time constant, its settling time after a step input and its static error(s).

This paper aims to highlight such changes and formulate conclusions about the advantages and disadvantages of using a certain ENCU within the control structure of a jet engine, even from the pre-design stage.

The first studied ENCU is hydro-mechanical-type (HMEN), as presented in [6], while the second one is pneumatic-hydraulic-type (PHEN presented in [7]), both ENCUs being used by aircraft jet engines with variable exhaust opening area.

The way in which these two controllers behave in the engine assembly is obviously different and, for their choice in the pre-design phase, a study is necessary to highlight how the engine would behave as an object subject to control under the conditions of ENCU embedding with the other controllers of the engine.

3. HYDRO – MECHANICAL - TYPE ENCU

A hydro-mechanical ENCU with complex structure and operation is the one studied in [6], depicted in Fig.1. In fact, this is a tracking (a "follower") system, which provides an opening of the exhaust nozzle depending on the position of the engine throttle (in other words, with respect to the power lever angle PLA).

The described ENCU operates with respect to the throttle's position (assured by the 1-lever rotation angle θ, equal to the PLA). Nozzle's flaps have profiled outer contours (as seen in Fig 1, position 32). When the actuator's rod (26) moves, it presses its 30-roll on this contour, determining nozzle flaps' opening.

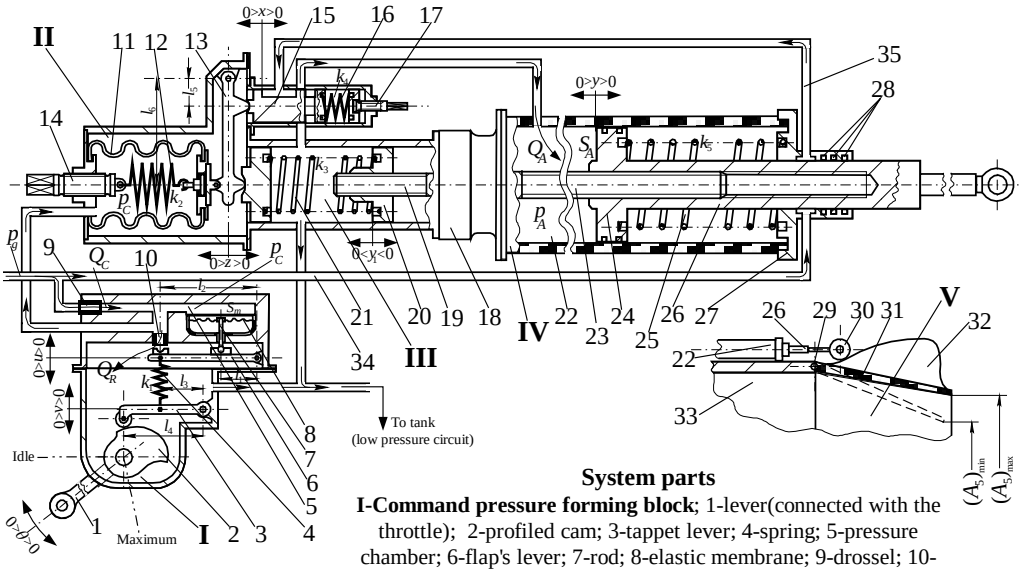

System parts

I-Command pressure forming block; 1-lever(connected with the throttle); 2-profiled cam; 3-tappet lever; 4-spring; 5-pressure chamber; 6-flap's lever; 7-rod; 8-elastic membrane; 9-drossel; 10-nozzle drossel; II-Slide-valve's command block; 11-silphon; 12-silphon's spring; 13-slide-valve's lever; 14-adjusting bolt;15-slide-valve; 16-slide-valve's spring; 17-adjusting bolt; **III-Position transducer**; 18-planetary reducing gear; 19-screw with thread on the left; 20-nut; 21-transducer's spring; **IV-actuator**; 22-hydraulic cylinder; 23-screw with thread on the right; 24-piston with nut; 25-actuator's spring; 26-actuator's rod; 27-lid; 28-sealing rings; **V-exhaust nozzle**; 29-knuckle; 30-pressing roll; 31-volet (flap); 32-profiled contour; 33-exhaust tube; 34,35-supplying pipes;

FIG. 1 Hydro-mechanical ENCU"s constructive and operational diagram [6]

Nozzle's opening log law $A_5 = A_5(\theta)$, determined by considerations of engine's gas-dynamics, is provided through 2-cam profile, which is connected to ENCU's lever. In fact, the gas-dynamics of the jet-engine imposes, at each engine regime (at each position of the throttle and at each spool speed), a certain value of the nozzle opening, and the cam profile is built in such a way as to realize the law thus determined; this is why it is said that the opening of the exhaust nozzle follows the position of engine's throttle, so ENCU is a tracking system.

Hydro-mechanical ENCU's linear adimensional simplified mathematical model was determined in [6], based on non-linear motion equations, linearised using finite differences method and brought to an adimensional form by favorable dividing. After Laplace transformation applying, one had obtained ENCU's mathematical model's usable form, which consists of the following equations:

$$\bar{v} = k_\theta \bar{\theta}, \tag{1}$$

$$\bar{u} = k_{uc}\bar{p}_C - k_{uv}\bar{v}, \tag{2}$$

$$\bar{p}_C = k_u\left(\tau_u \mathrm{s} + 1\right) - k_{gp}\bar{p}_g, \tag{3}$$

$$\bar{x} = k_{xc}\bar{p}_C - k_{xy}\bar{y}, \tag{4}$$

$$\bar{p}_A = k_{gA}\bar{p}_g + k_x\bar{x} - \tau_y \mathrm{s}\bar{y}, \tag{5}$$

$$\bar{y} = \frac{k_{yA}}{T_y^2\mathrm{s}^2 + 2\omega_0 T_y \mathrm{s} + 1}\bar{p}_A, \tag{6}$$

together with $\bar{A}_5 = k_{5y}\bar{y}$ - the adimensional equation of the nozzle's opening. The above-used coefficients of the mathematical model have the form presented in [6]. Based on these equations, ENCU's block diagram with transfer functions was built and depicted in Fig. 2.

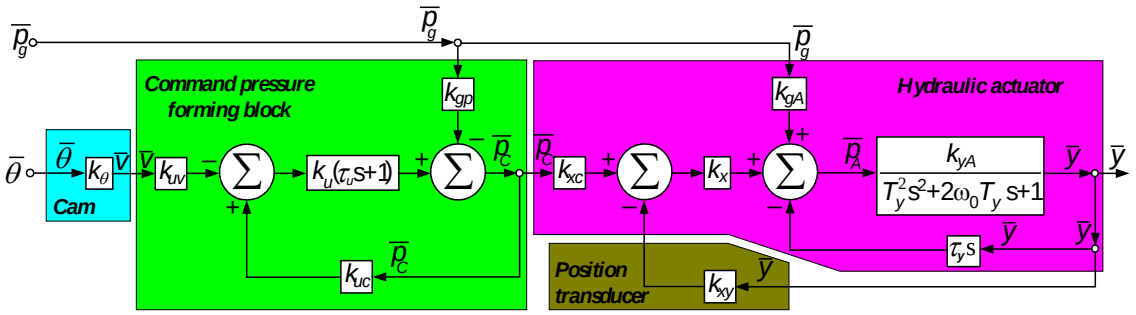

FIG. 2 Hydro-mechanical ENCU's block diagram with transfer functions [6]

One may observe that ENCU has two inputs: the power lever angle (PLA) $-\theta$, as well as the supplying hydraulic pressure $-p_g$. However, as far as the hydraulic pump is driven by the engine's spool and is assisted by a constant pressure valve, one may assume that p_g is nearly constant and its behavior as input becomes irrelevant, so ENCU's transfer function, determined based on its mathematical model, is:

$$H_\theta(\mathrm{s}) = \frac{\tau_{u\theta}\mathrm{s} + \rho_\theta}{(\tau_{yA}\mathrm{s}+1)(\tau_{uA}\mathrm{s}+1)}, \tag{7}$$

where the coefficients' expressions are $\tau_{yA} = \frac{k_5 k_{yA}\tau_y + \xi}{k_5(1+k_{yA}k_x k_{xy})}$, $\tau_{uA} = \frac{k_u k_{uc}\tau_u}{k_u k_{uc}-1}$, $\tau_{u\theta} = \frac{k_{yA}k_x k_{xc}k_u k_{uv}k_\theta \tau_u}{(k_u k_{uc}-1)(1+k_{yA}k_x k_{xy})}$ and $\rho_\theta = \frac{k_\theta - k_{yA}k_{gA}k_x k_{xc}k_{uc}k_{uv}}{(k_u k_{uc}-1)(1+k_{yA}k_x k_{xy})}$, as presented in [6].

A particular form of the model, for an ENCU belonging to a VK-1A-type engine, is the one used in [6] for quantitative evaluation:

$$\bar{A}_5(t) = \frac{0{,}0712\times(0{,}0422\mathrm{s}+0{,}1025)}{(0{,}1474\mathrm{s}+1)(0{,}6376\mathrm{s}+1)}\bar{\theta}(t)\ . \tag{8}$$

4. PNEUMATIC – HYDRAULIC – TYPE ENCU

This type of ENCU (presented and studied in [7]) consists of three main parts: I – the exhaust nozzle, II – the hydraulic actuator (with inner rigid feedback) and III – the pneumatic pressure ratio transducer (with flow rate corrector).

As Fig. 3 shows, the variable exhaust nozzle is equipped with overlapping petals (1), which have the outer contour (2) designed to assure nozzle's opening law, as the engine's operating gas-dynamic conditions request ([3], [10]). Hydraulic actuator's rod (6), equipped at the free end with a pressing roller (4), interacts, during its movement, with the outline of the petals and forces them to overlap more or less, leaving a smaller or a larger nozzle opening (between extreme positions of $A_{5\min}$ and $A_{5\max}$). The actuator's slide-valve (10) is commanded by the pressure ratio transducer's rod (16), in order to assure the gas-dynamic conditions behind the turbine as to maintain constant the turbine pressure drop (constant pressure ratio p_3^*/p_4^*, where p_3^* and p_4^* are hot gases total pressures before/behind the turbine).

The pressure transducer has two active chambers - one for p_4^* and the other one for the reference pressure p_R, separated by an elastic metallic membrane (15); it has also two variable fluidic resistances – one for the supply (20) and the other for the discharge (17), meant to assure the reference pressure value. However, as long as burned gas temperature T_3^* at turbine's inlet is high, one uses instead of p_3^* the air pressure behind the compressor p_2^* ($p_3^* = \sigma_{cb}^* p_2^*$, where $\sigma_{cb}^* < 1$ is the total pressure loss coefficient inside the combustor) to protect the pressure transducer; one may also use another smaller air pressure signal, from an intermediate stage of the compressor, to avoid the excessive mechanical charge of transducer's membrane. Transducer's flow rate corrector (18) operates similarly to the transducer, but it has as inputs air pressures before and behind engine's compressor; it has two pressure chambers (for air pressure in front of the compressor and for the correction pressure), an elastic membrane (19) and two variable fluidic resistances (21 and 22). The 22-resistance is an adjustable-one, and serves to set the suitable correction pressure value, during the program of testing and adjustment operations on ground testing rig, before ENCU enters service.

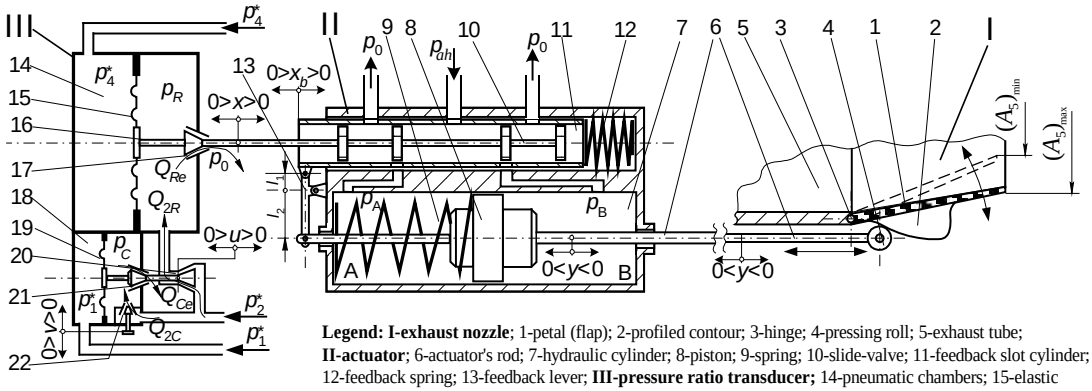

Legend: I-exhaust nozzle; 1-petal (flap); 2-profiled contour; 3-hinge; 4-pressing roll; 5-exhaust tube; **II-actuator**; 6-actuator's rod; 7-hydraulic cylinder; 8-piston; 9-spring; 10-slide-valve; 11-feedback slot cylinder; 12-feedback spring; 13-feedback lever; **III-pressure ratio transducer;** 14-pneumatic chambers; 15-elastic membrane; 16-transducer's rod; 17-profiled fluidic resistance; 18-flow rate corrector; 19-corrector's elastic membrane; 20-transducer's variable fluidic resistance; 21- corrector's variable fluidic resistance (connected to 20-resistance); 22- adjustable fluidic resistance (adjusting screw driven).

FIG. 3 Pneumatic – hydraulic ENCU constructive and operational diagram [7]

ENCU's simplified mathematical model, as determined in [7], consists of linearised adimensional equations of pressure ratio's transducer with flow rate corrector (the pneumatic component), of hydraulic actuator and, obviously, of nozzle's opening:

$$\overline{p}_C = \frac{1}{\tau_C \mathrm{s} + 1}\left[k_{2C}\,\overline{p}_2^* - k_{uC}\left(\tau_u \mathrm{s} + 1\right)\overline{u}\right], \tag{9}$$

$$\overline{p}_1^* - \overline{p}_C = \frac{1}{k_{pu}}\,\overline{u}\,, \tag{10}$$

$$\overline{p}_R = \frac{1}{\tau_R \mathrm{s} + 1}\left[k_{2R}\,\overline{p}_2^* + k_{uR}\,\overline{u} - k_{xR}\left(\tau_x \mathrm{s} + 1\right)\overline{x}\right], \tag{11}$$

$$\overline{p}_4^* - \overline{p}_R = \frac{1}{k_{px}}\,\overline{x}\,, \tag{12}$$

$$\overline{y} = \frac{1}{\tau_s \mathrm{s} + \rho_s}\,\overline{x}\,, \tag{13}$$

$$\overline{A}_5 = k_{yA}\,\overline{y}\,, \tag{14}$$

with the notations explained in [7]:

$$\tau_s=\frac{S_p y_0}{\mu_b x_0}\sqrt{\frac{\rho_h}{p_{ah}-p_0}},\ \rho_s=\frac{k_{e9}y_0}{2S_p\sqrt{p_{ah}-p_0}}+\frac{y_0}{x_0}\frac{l_1}{l_2},\ k_{yA}=\frac{y_0}{A_{50}}\left(\frac{\partial A_5}{\partial y}\right)_0,\ \tau_R=\frac{\beta V_{R0}}{k_{pR}},$$

$$\tau_x=\frac{S_{mR}}{2k_{Rx}},\ k_{2R}=\frac{k_{R2}p_{20}^*}{k_{pR}p_{R0}},k_{xR}=\frac{k_{Rx}x_0}{k_{pR}p_{R0}},\ k_{px}=\frac{S_{mR}p_{R0}}{k_{e1}x_0},k_{pR}=\frac{A_{170}K_a}{\sqrt{T_{20}^*}},\ k_{R2}=\frac{A_{22}K_a}{\sqrt{T_{20}^*}},$$

$$\tau_C=\frac{\beta V_{C0}}{k_{pC}},\ k_{Rx}=\frac{\pi K_a p_{R0}}{2\sqrt{T_{20}^*}}\tan\alpha\left[x_0\tan\alpha-(d_2-d_1)\right],\ k_{2C}=\frac{k_{C2}p_{20}^*}{k_{pC}p_{C0}},$$

$$k_{C2}=\frac{A_{21}K_a}{\sqrt{T_{20}^*}},\ k_{uC}=\frac{k_{Cu}u_0}{k_{pC}p_{C0}},\tau_u=\frac{S_{mC}}{2k_{Cu}},\ k_{pu}=\frac{S_{mC}p_{C0}}{k_{e2}u_0},k_{pC}=\frac{A_{c0}K_a}{\sqrt{T_{20}^*}}$$

$$k_{Cu}=\frac{\pi K_a p_{C0}}{2\sqrt{T_{20}^*}}\tan\alpha_2\left[u_0\tan\alpha_2-(d_4-d_3)\right],\ k_{uR}=\frac{\pi K_a p_{R0}}{2\sqrt{T_{20}^*}}\tan\alpha_3\left[u_0\tan\alpha_3-(d_6-d_5)\right],$$

χ_a – air's adiabatic exponent, R_a – air's gas constant, $K_a=\sqrt{\frac{\chi_a}{R_a}\left(\frac{2}{\chi_a+1}\right)^{\frac{\chi_a+1}{\chi_a-1}}}$. (15)

Based on the above-presented model, the ENCU's block diagram with transfer functions was built up and depicted in Fig. 4.

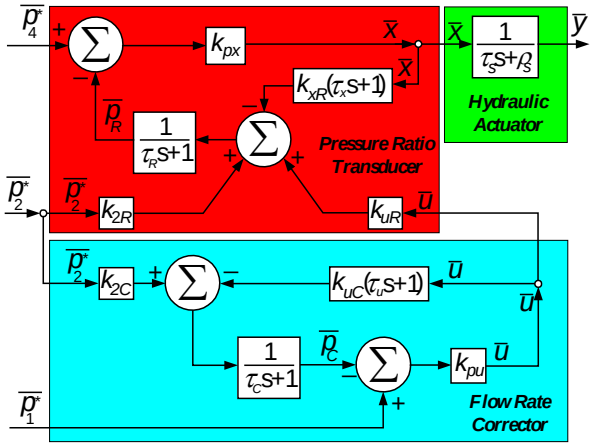

FIG. 4 Pneumatic-hydraulic ENCU block diagram with transfer functions

ENCU has three inputs (the pressure in front of the compressor p_1^*, behind the compressor p_2^* and behind the turbine p_4^*) and one output (actuator's rod displacement y). In terms of p_1^*, it brings the influence of the aircraft (and engine) flight regime, so, for constant flight regime $\overline{p}_1^*=0$ its influence becomes irrelevant; the other ENCU's inputs are, in fact, aircraft engine's outputs, so ENCU brings another feedback inside engine's mathematical model.

5. AIRCRAFT ENGINE CONTROL ARCHITECTURE

Any aircraft jet engine has its own control system, more or less complex, depending on its architecture, its level of performance and its specific field of use. The embedding of an ENCU into a certain control architecture depends on its own operational properties (such as its inputs parameters, which often are other engine's outputs).

An aircraft jet-engine, as controlled object, is a MIMO system ([5], [9], [11]), whose control parameters (inputs) are: the fuel flow rate (for the basic engine and for the afterburning, if operational) and the nozzle's opening. Other inputs may appear, for example if the engine is fitted with thrust augmentation system through coolant injection, when the coolant flow rate may become an input parameter too.

However, from pilot's point of view, the engine is a SISO, which has a single input – the power lever angle (throttle's position) and a single output – the thrust. So, any control architecture must use sub-controllers, which must give the level of the main inputs (fuel flow rate and nozzle opening) with respect to engine's throttle position (PLA).

ENCU's embedding into a control architecture is formally depicted in Fig. 5.

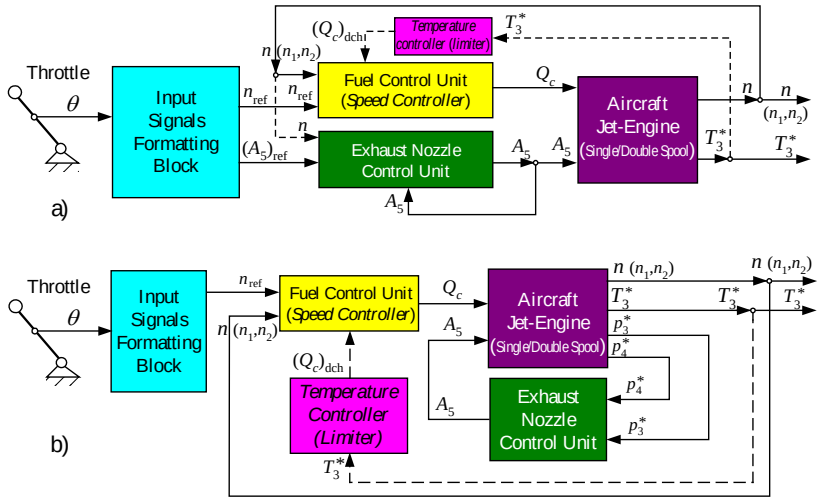

FIG. 5 Jet-engine's embedded control architecture

The hydro-mechanical ENCU's embedding is much more simple, as Fig. 5.a) shows, because it is necessary only a simple signal forming block for the tracking of PLA $-\theta$, while the pneumatic-hydraulic ENCU's embedding is more complex, as. Fig. 5.b) shows, because of the presence of the pressure intakes for the input pressures (p_2^* and p_4^*), which are, in fact, engine's secondary outputs.

Along with the nozzle controllers, there must be also fuel flow rate controllers (fuel control units – FCU), which, as shown in [11], have effects both on the engine speed(s), as well as on the temperature of the combustion chamber. The operating principles of any FCU are based on the control of the engine speeds, having these as quantities used in the control loops (thereby creating internal feedbacks).

The speed control is based on the fact that the thrust of a jet-engine is always proportional to its spool rotational speed and, as long as the thrust is impossible to be correctly measured and inserted into a control loop, the spool speed can successfully replace the thrust, being a relevant and easily measurable parameter ([9], [10]). Consequently, control units embedding has different complexity levels; for example: a two-spool jet-engine's FCU has the fuel pump driven by the high-pressure shaft, while the speed transducer is connected to the low-pressure shaft, which makes of both engine's speeds important controlled parameters (as Fig. 5 highlights).

One has chosen for the study a FCU similar to the one described and studied in [5] designed for a double spool jet engine consisting of: a main fuel pump (driven by the high pressure spool), a hydraulic-type actuator (fitted with rigid feedback) and a speed transducer (driven by the low-pressure spool). This model of FCU may be used for turbofans too.

Following equation is describing the mathematical model of the FCU and in Fig. 6 is depicted FCU's block diagram with transfer functions:

$$\overline{Q_c} = k_{pn}\overline{n}_2 - \frac{k_{py}k_{es}}{\tau_s \mathrm{s} + \rho_s}\overline{n}_1 + \frac{k_{py}k_u k_{u\theta}}{\tau_s \mathrm{s} + \rho_s}\overline{\theta}, \tag{16}$$

which may be used for quantitative determinations in the following form

$$\overline{Q_c}(t) = 0.5\overline{n}_2(t) - \frac{0.274\overline{n}_1(t) - 0.782\overline{\theta}(t)}{0.114\mathrm{s} + 0.815}. \tag{17}$$

It must be stated that, for single-spool jet-engines, the fuel pump and the speed transducer are driven by the engine's shaft through engine's gear, so they both have the same rotational speed; consequently, for such an FCU $\overline{n}_1 = \overline{n}_2 = \overline{n}$ and its mathematical model becomes:

$$\overline{Q_c} = \frac{\left(k_{pn}\tau_s \mathrm{s} + k_{pn}\rho_s - k_{py}k_{es}\right)\overline{n} + k_{py}k_u k_{u\theta}\overline{\theta}}{\tau_s \mathrm{s} + \rho_s}, \tag{18}$$

$$\text{or } \overline{Q_c}(t) = \frac{\left(0.057\mathrm{s} + 0.1335\right)\overline{n}(t) + 0.782\overline{\theta}(t)}{0.114\mathrm{s} + 0.815}. \tag{19}$$

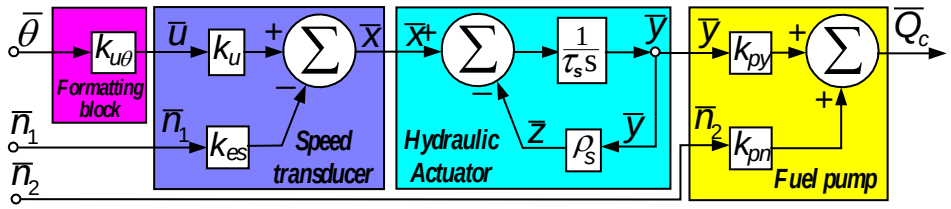

FIG. 6 Block diagram with transfer functions of the fuel control unit [5]

Whatever the architecture of the jet-engine control system, there must also exist an auxiliary control unit to limit the combustor temperature to an admissible value (as Fig. 5 shows), which, however, also acts on the fuel's mass flow rate (through the additional discharge $(Q_c)_{\mathrm{dch}}$ flow), so it will somehow be integrated into the FCU.

Both embedded control systems depicted in Fig. 5 were studied for three types of jet engines: a) a single-spool single-jet engine (SJE); b) a two-spools single-jet engine (TJE); c) a low by-pass turbofan (also a two-spools engine, TFE).

For quantitative determinations one has used for each one of the above-presented engines the equations established in [5] and [11], as follows:

-for SJE: $$\overline{n}(t) = \frac{1.2606\overline{Q}_c(t) + 0.476\overline{A}_5(t)}{2.0859\mathrm{s} + 5.1015}, \tag{20}$$

$$\overline{T_3^*}(\mathrm{s}) = \frac{\left(1.3799\,\mathrm{s} + 2.3888\right)\overline{Q}_c(t) + \left(0.339\mathrm{s} + 1.211\right)\overline{A}_5(t)}{2.0859\mathrm{s} + 5.1015}, \tag{21}$$

-for TJE: $$\overline{n}_1(t) = \frac{\left(0.061\mathrm{s} + 0.174\right)\overline{Q}_c(t) + \left(0.027\mathrm{s} + 0.118\right)\overline{A}_5(t)}{0.1395\mathrm{s}^2 + 0.761\mathrm{s} + 1.227} \tag{22}$$

$$\overline{n}_2(t) = \frac{\left(0.102\mathrm{s} + 0.351\right)\overline{Q}_c(t) + 0.1081\overline{A}_5(t)}{0.1395\mathrm{s}^2 + 0.761\mathrm{s} + 1.227}, \tag{23}$$

$$\overline{T}_3^*(t)=\frac{(0.04s^2+0.0217s+0.198)\overline{Q}_c(t)+(0.054s+0.223)\overline{A}_5(t)}{0.1395s^2+0.761s+1.227}, \quad (24)$$

-for TFE: $$\overline{n}_1(t)=\frac{(0.208s+0.341)\overline{Q}_c(t)+(0.274s+0.242)\overline{A}_5(t)}{0.414s^2+4.181s+3.377} \quad (26)$$

$$\overline{n}_2(t)=\frac{(0.294s+0.514)\overline{Q}_c(t)+(0.412s+0.366)\overline{A}_5(t)}{0.414s^2+4.181s+3.377}, \quad (27)$$

$$\overline{T}_3^*(t)=\frac{(0.018s^2+0.194s+0.285)\overline{Q}_c(t)+(0.382s+0.436)\overline{A}_5(t)}{0.414s^2+4.181s+3.377}. \quad (28)$$

It can be seen that the influence of the exhaust nozzle opening is different for each type of engine, so incorporating the ENCU into the control system is more complex the more complex the engine design.

6. COMPARISON BETWEEN CONTROL SYSTEMS' BEHAVIORS

Embedded control systems' quality was estimated studying their step responses. For comparison, any studied jet-engine was considered, alternately, as fitted with both types of nozzle (hydro-mechanical HMEN and pneumo-hydraulic PHEN). Any engine has, in fact, a single input (see Fig. 5), which is the PLA-parameter $\overline{\theta}$, so one has considered for study PLA step input (assumed as a sudden throttle displacement, from idle to maximum). One has also neglected the other possible input parameter $\overline{p}_1^*$, which, otherwise, gives the influence of the flight regime.

As main output parameters one has selected engines' spool rotational speed parameters ($\overline{n}$ for the single spool single-jet engine SJE, while for double spool engines TJE and TFE - $\overline{n}_1$ - low pressure spool speed and $\overline{n}_2$ - high pressure spool speed); a relevant secondary output parameter was also considered for study – the combustion chamber's temperature parameter $\overline{T}_3^*$.

For quantitative determinations one has used the formulas (8), (18) and (19) to (28). Simulation results are graphically depicted in Fig. 7 – for SJE, in Fig. 8 – for TJE, while in Fig. 9 – for TFE. Figures a) are reserved for engines' speed(s) behaviors, while figures b) show temperatures' behaviors.

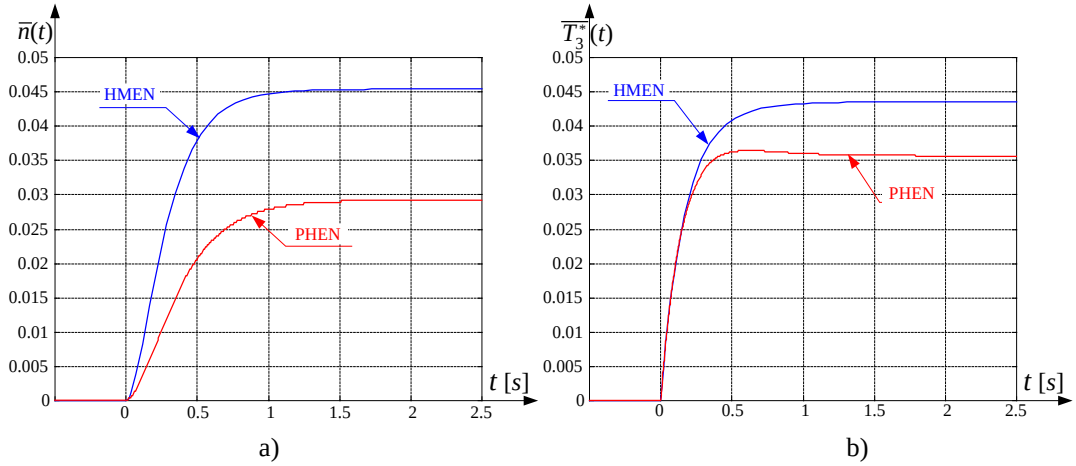

FIG. 7 Step responses of speed and temperature parameters for a single-spool single-jet engine SJE

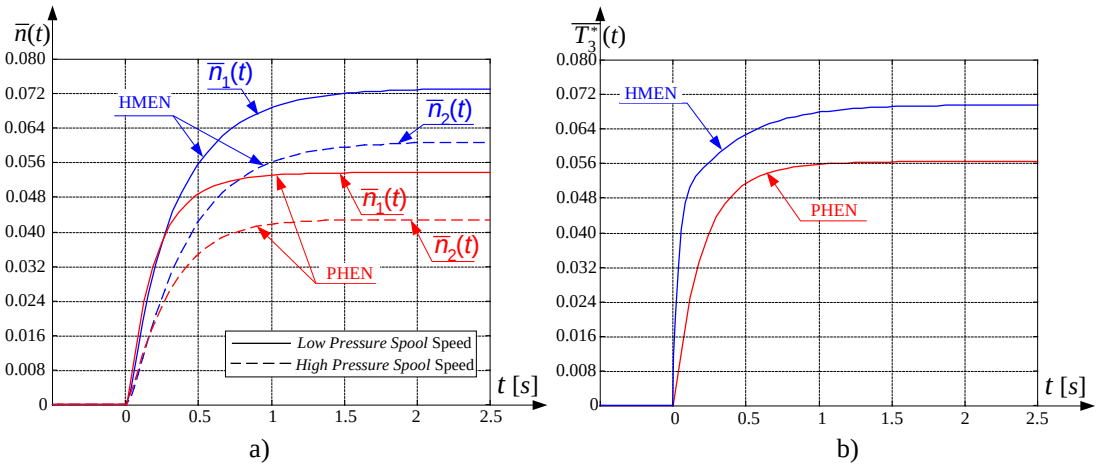

FIG. 8 Step responses of speed and temperature parameters for a two spools single-jet engine THE

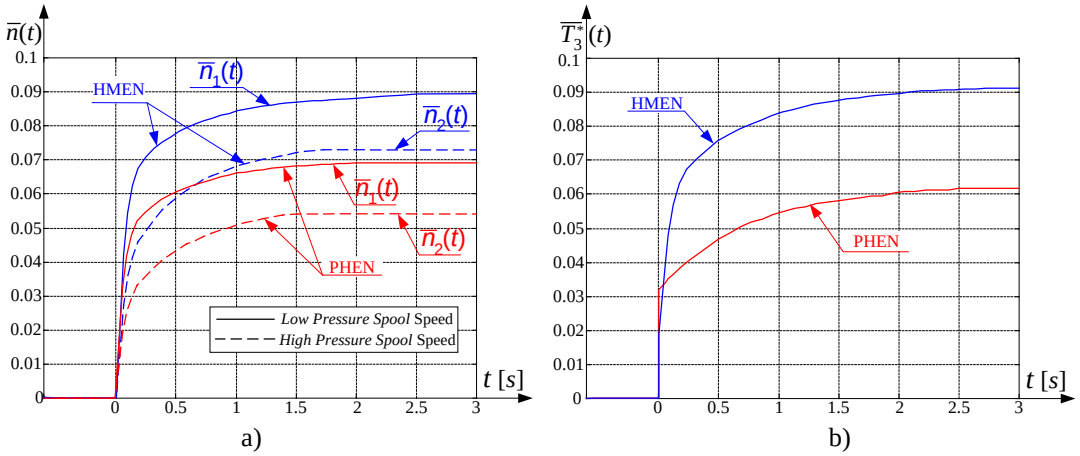

FIG. 9 Step responses of speed and temperature parameters for a low by-pass turbofan TFE

CONCLUSIONS

As all above-presented figures show, whatever the engine and whatever the nozzle version, the embedded control systems ensure asymptotically stable behavior of the engines, with settling times and static errors of acceptable values. However, there are certain differences between the behavior of the two types of equipment (from static error and settling times values point of view), which, highlighted, lead to conclusions regarding which nozzle controller is recommended for a certain type of jet-engine.

One has studied two different ENCUs as part of embedded control systems for different jet-engines (single-spool or twin-spool single-jet aircraft engines).

For a SJE, the use of HMEN produces higher values of the static errors (both for the speed and for the combustor's temperature parameters) than PHEN, but lower settling times values. In addition, the use of PHEN produces a small initial temperature overshoot (as Fig. 7.b) shows), which could be a disadvantage, although the subsequent stabilization is still asymptotic. A possible cause might be the presence of the pneumatic equipment.

As for both twin-spool engines (TJE and TFE), figures 8 and 9 show for all studied parameters similar behaviors. For the two-spool single-jet engine (TJE), fig. 8 shows that, from spools' speed point of view, HMEN offers smaller static errors (5.4% for n_1 and 4.8% for n_2) than PHEN (9% for n_1 and 6.8% for n_2) and smaller settling times (1.5 s,

smaller than 2 s); combustor temperature parameter has smaller static error for PHEN (5.6%) than for HMEN (7%), but near same settling times (around 1.5 s).

For the low-bypass turbofan (twin-spool-type too), figures 9 prove high similarity to TFE from spool speeds point of view, but higher static errors and settling times. For $\overline{n}_1$ HMEN offers 9% static error and 2.6 s settling time, while for $\overline{n}_2$ - 7% static error and 1.7 s settling time, comparing to PHEN, where $\overline{n}_1$ has 6.8% static error and 1.8 s settling time and

$\overline{n}_2$ has 5.4% static error and 1.4 s settling time; temperature parameter has, in both cases, initial sudden increases (smaller for HMEN), but asymptotic stabilization, with 9.2% static error for HMEN and 6.3% for PHEN and similar settling times (2.7 s for HMEN and 2.5 s for PHEN).

As a final conclusion, it can be stated that PHEN offers better performance than HMEN to the engine it equips, especially for twin-spools engines, these becoming faster when accelerating and stabilizing at values of the controlled parameters closer to those assumed by design and calculation.

However, the final decision belongs to the engine designer, who must also take into account the aspects of efficiency and reliability in operation and, last but not least, the benefit/cost ratio, as well as the aspects related to maintenance.

REFERENCES

[1] J. D. Mattingly, *Elements Of Gas Turbine Propulsion*. McGraw-Hill, New York, 1996;
[2] V. Pimsner, *Air-breathing Jet Engines. Processes and Characteristics*, Bucharest, Didactic and Pedagogic Publishing, 1983;
[3] P. G. Hill, C. Peterson, *Mechanics and Thermodinamics of Propulsion*. Addison - Wesley Publications, New York, 1993;
[4] C. Berbente and N. V. Constantinescu, *Gases Dynamics*, vol. I, II. Politehnica University in Bucharest Inprint, 1985;
[5] A. N. Tudosie, *Aerospace Propulsion Systems Automation*. University of Craiova Inprint, 2005;
[6] A. N. Tudosie, Aircraft Jet Engine Exhaust Nozzle Hydro-Mechanical Automatic Control System, in *Proceedings of International Conference of Scientific Paper AFASES 2012*, Brasov, May 24-26, 2012, pp. 753-760;
[7] A. N. Tudosie, Aircraft Jet Engine Exhaust Nozzle Controller Based on Turbine Pressure Ratio Sensor with Micro-jet System, in *Proceedings of International Conference on Applied and Theoretical Electricity ICATE 2012*, Craiova, October 25-27, 2012, DOI: 10.1109/ICATE.2012.6403464;
[8] I. Aron, A. Tudosie, Jet Engine Exhaust Nozzle's Automatic Control System, in *Proceedings of the 17th International Symposium on Naval and Marine Education*, sect. III, pp 36-45, May 2001;
[9] C. Rotaru, I. R. Edu, M. Andres-Mihaila and P. Matei, Applications of multivariable control techniques to aircraft gas turbine engines, in *Review of Air Force Academy*, no.2 (26), 2014, pp. 45-50;
[10] L. C. Jaw, J. D. Mattingly, *Aircraft Engine Controls: Design, System Analysis, and Health Monitoring*, AIAA Education Series, 2009;
[11] A. N. Tudosie, *Aircraft Gas-Turbine Engine's Control Based on the Fuel Injection Control*. In Max Mulder's Aeronautics and Astronautics, INTECH Open, 2011, DOI 10.5772/17986.